

Diammonium hydrogenphosphate treatment on dolostone: the role of Mg in the crystallization process

Elena Possenti^{1,*}, Claudia Conti¹, G. Diego Gatta², Marco Realini¹ and Chiara Colombo¹

¹ Istituto per la Conservazione e la Valorizzazione dei Beni Culturali (ICVBC), Consiglio Nazionale delle Ricerche (CNR), Via R. Cozzi 53, 20125 Milan, Italy; possenti@icvbc.cnr.it, c.colombo@icvbc.cnr.it, c.conti@icvbc.cnr.it, m.realini@icvbc.cnr.it

² Dipartimento di Scienze della Terra, Università degli Studi di Milano, Via Botticelli 23, 20133 Milan, Italy; diego.gatta@unimi.it

* Correspondence: possenti@icvbc.cnr.it; Tel.: +39-02-66173386

Received: date; Accepted: date; Published: date

Abstract: The diammonium hydrogenphosphate (DAP, $(\text{NH}_4)_2\text{HPO}_4$) reaction with calcite has been extensively investigated. The availability of free calcium ions in the reaction environment has been acknowledged as a crucial factor in the crystallization of calcium phosphates with a high (hydroxyapatite, Ca/P 1.67) or low Ca/P molar ratio (dicalcium phosphate dihydrate, Ca/P 1.00; octacalcium phosphate, Ca/P 1.33). On the contrary, no data are available on the DAP interaction at room temperature with dolomite in terms of reaction mechanism and composition of the reaction products. Here, a multi-analytical approach based on SEM-EDS and X-ray powder diffraction before and after heating treatments is proposed to explore how the formation of calcium phosphates occur on Mg-enriched substrates and if the presence of magnesium ions during the reaction influences the crystallization process of calcium phosphates. The DAP reaction with polycrystalline dolomite gives rise to the formation of struvite and of poorly crystalline hydroxyapatite. Calcium and magnesium ions mutually interfered in the crystallization of magnesium and calcium phosphates, respectively, whose effects influence the properties (size, micro-morphology, composition and crystallinity) of the newly-formed phases.

Keywords: calcium phosphate; hydroxyapatite; magnesium phosphate; struvite; dolomite; consolidating treatment; cultural heritage; ammonium phosphate

1. Introduction

Diammonium hydrogenphosphate (DAP, $(\text{NH}_4)_2\text{HPO}_4$) is a promising inorganic consolidating treatment for decayed carbonatic stones [1–4]. The DAP consolidating treatment aims at restoring the stone matrix through a partial transformation of the original material in newly-formed phosphate phases. Ideally, crystalline hydroxyapatite (HAP, $\text{Ca}_5(\text{PO}_4)_3\text{OH}$) is formed by combining calcium ions of the substrate with phosphate groups of the reagent [5,6].

The DAP reaction with calcite (CaCO_3) of carbonatic stones has been extensively investigated during the last years, [7,8] and recent findings showed that the DAP reaction with polycrystalline calcite of carbonatic stones is non-stoichiometric [9], which implies that many crystalline phases may form in complex mixtures with a nanocrystalline and/or partially-substituted HAP [1,5,6,9–12]. Furthermore, it has been demonstrated that the composition of the new phases depends on several variables, as *e.g.*, the reaction condition (pH, ion strength), the stone substrate (lithotype, microstructure) and the treatment protocol (duration, application method, DAP molarity) [10,13–16].

The DAP reaction in presence of low amount of calcium ions (*e.g.*, when DAP is used with a low molarity [9] or on calcite substrates with Mg-containing veins [17]) follows a different crystallization process. In particular, the availability of free calcium ions is a crucial factor in the crystallization; phases with a low Ca/P molar ratio (*e.g.*, dicalcium phosphate dihydrate DCPD $\text{CaHPO}_4 \cdot 2\text{H}_2\text{O}$, Ca/P molar ratio 1.00, and octacalcium phosphate OCP $\text{Ca}_8(\text{HPO}_4)_2 \cdot 5\text{H}_2\text{O}$, Ca/P molar ratio 1.33), [13,14] are formed instead of HAP [9,18] (Ca/P molar ratio 1.67) in reaction environments with a low concentration of calcium ions.

Over the centuries, several carbonatic stones with magnesiatic nature have been used for artefacts and buildings. A crucial issue is the challenging conservation of Angera stone, a sedimentary dolostone widely used as ornamental lithotype in the North of Italy and severely affected by decay [19]. The literature on the investigation of DAP treatments applied to calcite-based materials of cultural heritage is progressively increasing, while, surprisingly, the DAP reaction with magnesium carbonates is still quite unexplored.

52 Clearly, the DAP reaction with magnesium carbonates is expected to give rise to a set of crystalline phases
53 different to those formed with calcium carbonate. However, even though the transformation of magnesium
54 carbonates into magnesium phosphates with hydrothermal conditions [20], or by calcination [21], is
55 well-known in literature, only a few studies investigated the carbonate-to-phosphate conversion at room
56 temperature [22,23], which normally is the operative condition of conservation treatments.

57 This study focuses, for the first time, on the reaction of polycrystalline dolomite with DAP solutions at
58 room temperature in order to explore how: i) DAP treatments react with dolostones; ii) the nucleation of
59 calcium phosphates occur in presence of Mg-enriched substrates; iii) the presence of magnesium and calcium
60 ions during the reaction influences the crystallization process of calcium and magnesium phosphates.

61 The DAP treatments were carried out by using DAP water solutions with two different molarities on
62 quarry specimens. The formation of specific crystalline phases and their diffusion inside the stone matrix are
63 investigated following a multi-analytical approach (SEM-EDS, X-ray diffraction before and after heating
64 treatments) and critically discussed.
65

66 2. Materials and Methods

67 2.1. Materials

68 The Angera stone, a dolostone quarried in the northern Italy (Piedmont) and widely used in the Lombard
69 architecture as ornamental building material since the Roman age, has been used for this study [24]. The
70 lithotype is characterized by a very fine grain size and a high porosity (18-26 %, depending on the Angera stone
71 variety). The stone is mainly composed of dolomite ($\text{CaMg}(\text{CO}_3)_2$) in association with a low fraction of clay
72 minerals and iron oxides [19,25–28].

73 The experiments were performed on the white variety of Angera stone, as it is the variety which undergoes
74 to the most severe decay processes in the environmental conditions. They were carried out on a set of freshly
75 quarried prismatic specimens (50×50×20 mm) in order to explore the crystallization of phosphates from DAP
76 solutions at room temperature on dolostones.

77 The Angera stone specimens were treated by a 0.76 M or of a 3.00 M aqueous solutions of DAP (CAS
78 Number 7783–28-0, assay $\geq 99.0\%$, reagent grade, Merck, Darmstadt Germany). The concentration 0.76 M
79 (corresponding to a 10% w/w) was selected on the basis of previous experiments [10] and on the consolidating
80 practice in conservation worksites [29]; the choice to include also 3.00 M concentration was suggested in
81 previous studies available in the literature [7,30], where this value was used to enhance the crystallization of
82 calcium phosphates. The consolidating DAP solution was applied by poultice (dry cellulose pulp, MH 300
83 Phase, Italy; ratio ~ 5:1 DAP solution: dry cellulose pulp), as it is one of the most common application methods
84 in the conservation field. The treatment time was 48 hours, during which the specimens were wrapped in a
85 plastic film to avoid the evaporation of the solvent. After 48 hours, the plastic film was removed and the
86 specimens were left drying at room temperature for other 24 hours with the poultice on top. The DAP poultice
87 was then removed and the specimens were rinsed three times by poultice made with deionised water and dried at
88 room temperature.
89

90 2.2. Methods

91 The crystalline phases of the Angera stone specimens before and after the consolidating treatments were
92 investigated by X-ray powder diffraction (XRD) in Bragg–Brentano geometry with a Panalytical X'Pert PRO
93 diffractometer, equipped with a PW 3050/60 goniometer, anti-scatter slit and divergence slit (1° and 1/2°
94 respectively), a PW3040/60 generator and a X'Celerator solid state detector PW3015/20 nickel filtered. The
95 samples were finely pulverised and spread on silicon zero background holders. The diffraction patterns were
96 collected with a Cu $K\alpha$ radiation source ($\lambda \sim 1.54 \text{ \AA}$), accelerating voltage 40 kV and electric current at the Cu
97 anode of 40mA, in the 2 Theta angular range 4.5 – 65 ° with a stepsize of 0.17 ° and time per step of 130 s.

98 A set of thermal treatments were carried out in order to fully explore the composition of the newly-formed
99 calcium phosphates, which showed ambiguously interpretable X-ray diffraction patterns. For this reason,
100 untreated and treated specimens were initially analysed at room temperature (rT); after that, the samples were
101 heated at 400 °C, 600 °C and 900 °C, and re-analysed at rT after each heating process. The selection of the

102 temperature steps used to investigate the *T*-induced “parent-to-product” phase transformation is driven by
103 literature data [9,16,31–36].

104 The micro-morphology of the specimens before and after the DAP treatments were investigated by
105 zenithal observations using a JEOL 5910 LV scanning electron microscope (SEM) coupled with energy
106 dispersive X-ray spectrometer (EDS) IXRF-2000 (0–20 keV) in high vacuum mode on carbon coated samples.

107
108

109 3. Results

110 3.1. Analysis of the newly-formed phases on Angera stone

111 Figure 1 shows the X-ray diffraction patterns of quarry Angera stone before and after the DAP
112 consolidating treatment. The XRD pattern of the untreated substrate shows well-defined peaks of dolomite
113 (main peak at 31.02° and secondary peaks at 24.13°, 33.61°, 35.33°, 37.42°, 41.18°, 44.96°, 50.59°, and 51.11°
114 of 2Theta, $\lambda = \text{Cu K}\alpha$) and weaker peaks of secondary minerals (quartz at 26.60° of 2Theta, phyllosilicates at
115 9.41° and 25.37°, feldspar at 26.96° and plagioclase at 27.48°).

116 The XRD patterns of Angera stone treated with 0.76 M and with 3.00 M DAP solution exhibit the
117 formation of magnesium phosphates and calcium phosphates. In fact, the XRD peaks of struvite
118 ($\text{MgNH}_4\text{PO}_4 \cdot 6\text{H}_2\text{O}$, peaks at 14.99°, 15.81°, 16.47°, 20.85°, 21.45°, 27.07° and 31.94°) and most likely apatite
119 (peak at ~25.90°) are revealed in mixture to the substrate phases.

120 The XRD peaks of struvite are sharp and well-resolved, indicating the formation of a well crystalline
121 phase, whereas the peak of the possible apatite is extremely weak and broad, most likely due to a poorly-ordered
122 structure. No other peaks ascribable to calcium phosphates are detectable in the XRD patterns, likely due to
123 overlapping with the peaks of other phases or to their severe weak intensity. Several calcium phosphate phases
124 have a peak at ~25.90° of 2Theta, as many of them are characterized by a similar crystalline structure (*e.g.*,
125 hydroxyapatite; calcium-deficient hydroxyapatite and its partially-substituted forms; octacalcium phosphate;
126 amorphous calcium phosphates, ACPs, $\text{Ca}_x\text{H}_y(\text{PO}_4)_z \cdot n\text{H}_2\text{O}$, with $n=3-4.5$ and 15-20% H_2O) [13,37–41]. The
127 peaks of struvite are more intense in the XRD patterns of the specimens treated with the 3.00 M DAP, while the
128 peak of the possible apatite is more visible in the 0.76 M ones.

129 The XRD pattern of the specimens treated with the 3.00 M DAP solution also shows evidence of residual
130 traces of the reagent (DAP peaks at 17.55°, 17.94°, 23.56°, 26.43°, 27.70°, 28.41° and 29.16°) and of
131 ammonium dihydrogen phosphate (ADP, $\text{NH}_4\text{H}_2\text{PO}_4$, at 16.63°), a by-product of the reaction; these two phases
132 are still present within the specimens despite they were rinsed. No peaks of DAP and ADP are detected on the
133 specimens treated with the 0.76 M DAP solution.

134 In order to further explore the microstructural-crystallographic feature of these poorly-ordered calcium
135 phosphate phases, a sequence of investigations were carried out by electron backscatter diffraction (EBSD),
136 FTIR and Raman spectroscopy. However, the outcomes of these supplementary techniques did not supply any
137 further information and their results are not reported in this paper.

138 In particular: i) for EBSD, it was not possible to obtain the XRD patterns of the investigated area due to the
139 poorly crystalline nature of the phases, their nanometric size and the boundary effects, deriving from the
140 alteration during the sample preparation of the interface between the new phases and the substrate; ii) for
141 Raman spectroscopy, phosphate phases have a weak Raman scatter, especially when submicrometric and/or
142 poorly ordered, and in mixture with carbonates (phases characterized by a very high Raman cross section); iii)
143 as for FTIR data, the superimposition of the characteristic stretching and bending PO_4 vibrational bands of both
144 the phosphate phases prevented their unambiguous identification.

145
146

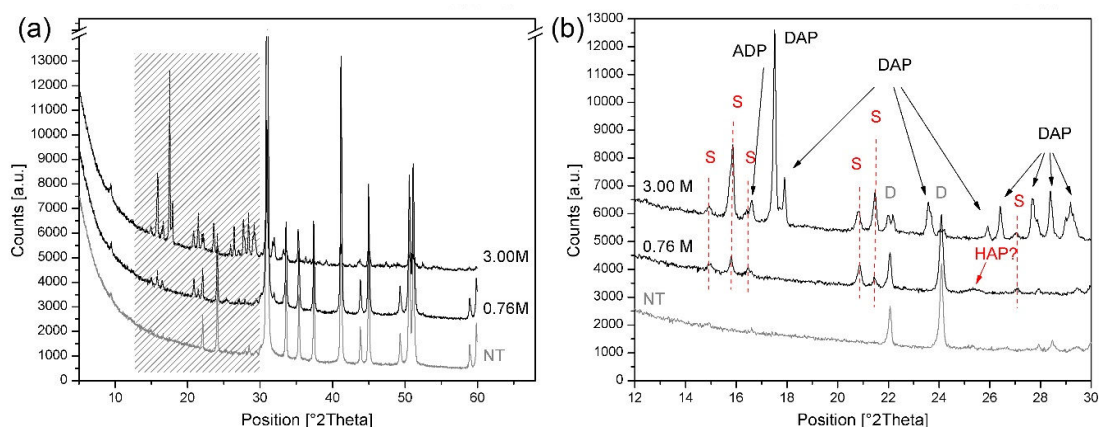


Figure 1. (a) XRD patterns of untreated Angera stone (NT) and Angera stone treated by poultice with a 0.76 M (0.760M) and 3.00 M (3.00M) DAP solutions. (b) Detail in the range 12-30 ° showing the phase variations occurred after the consolidation. D = dolomite, S = struvite, HAP? = possible hydroxyapatite, DAP = diammonium hydrogen phosphate, ADP = ammonium dihydrogen phosphate.

3.2. Micro-morphological investigations of the stone surface

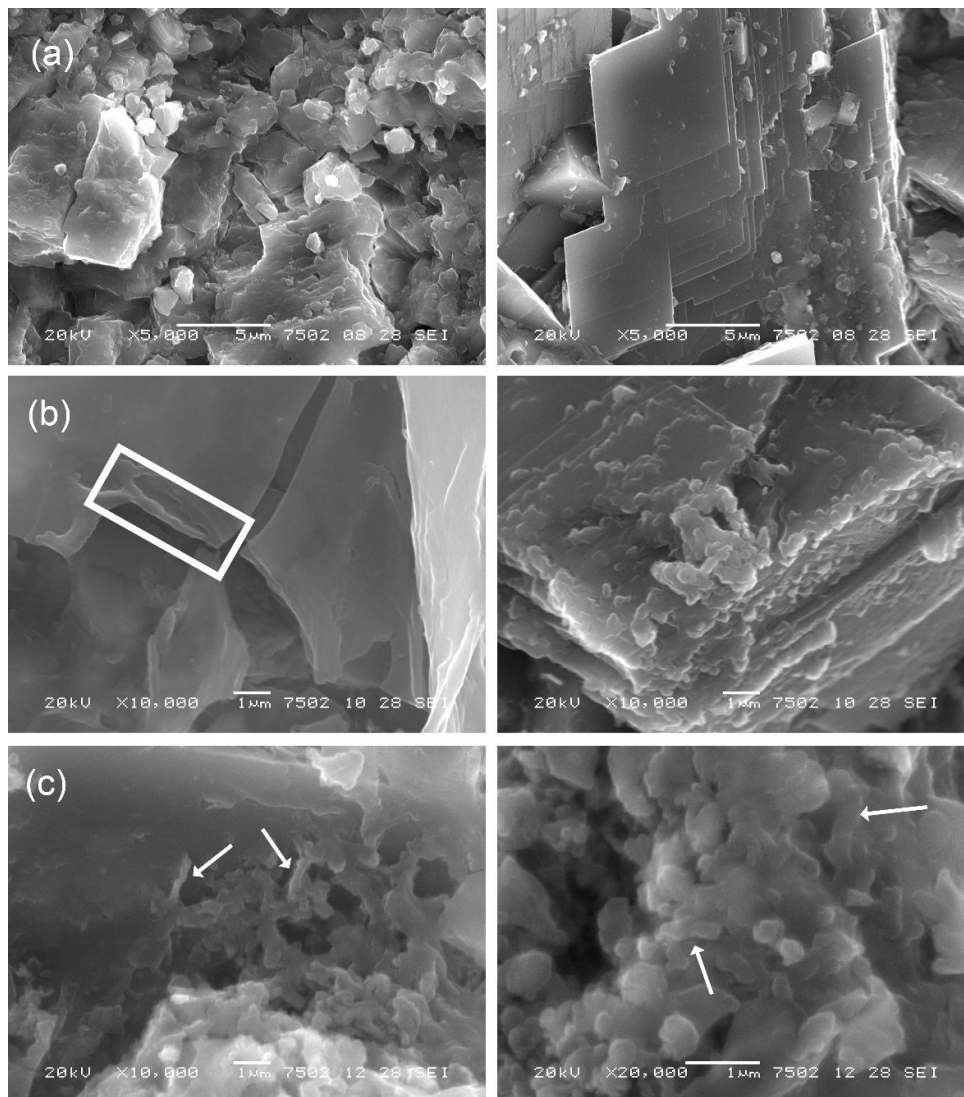
The micro-morphology of untreated Angera stone, showing the well-shaped rhombohedral crystals habit of dolomite is appreciable in Figure 2a, while that of the reacted dolomite is shown in Figures 2b and 2c. After the DAP treatments, the stone surface shows the presence of a newly-formed coating characterized by a pseudo-amorphous aspect. This coating is prevalently adherent to the stone matrix together with the crystallization of spherical particles agglomerates. Both of them cover the characteristic morphological features of the lithotype.

In the case of the specimens treated with the 0.76 M DAP solution, the newly-formed phases appear as a pseudo-amorphous thin film (thickness ~ 0.6 μm) that covers the micritic dolomite (Figure 2b, left). On the film profiles, an incipient formation of spherical particles in an elongated arrangement has been detected. On dolomite rhombohedral grains (dolomite crystal size ~ 15-20 μm), a shell of spherical crystallites having a bigger size is distinguishable (Figure 2b, right).

In the case of the specimens treated by DAP 3.00 M, the profiles of the dolomite crystals appear affected by pronounced corrosion marks, with the consequent crystal nucleation of spherical structures combined to form elongated chain individuals (detail of Figure 2c).

Phosphorous is detected by EDS microanalysis in correspondence of the crystals overgrown on the substrate and morphologically different from the dolomite grains of the substrate. By measuring these newly-formed phases, calcium, magnesium and phosphorous are always present, even though the ratio of their elemental abundance varies.

The SEM investigations suggest the presence of two different phosphates phases, a magnesium and a calcium phosphate which exhibit differences in morphology and particle size (Figure 2b and c). These phases (struvite and a possible apatite, as suggested by the XRD data) do not show their typical orthorhombic and rose-like morphologies [9,42]. However, on the basis of the XRD results and on literature data about the mutual influence of Ca^{2+} and Mg^{2+} ions on the size and habit of hydroxyapatite and struvite, it is possible to hypothesize the following correlation: i) the pseudo-amorphous aspect of the coating could be ascribed to nano-sized agglomerates of Ca-phosphate spherical particles; ii) the spherical particles (consistently in the range of 10–50 nm; dimension slightly affected by the treatment concentration) often characterized by an aggregate prismatic aspect (Figure 2c, right) could be correlated to the formation of magnesium phosphate nuclei.



181
182
183
184
185
186
187
188

Figure 2. SEM images of Angera stone. (a) untreated substrate, showing micritic dolomite on the left and bigger grains of well-shaped rhombohedral dolomite on the right; (b) treated lithotype after the poultice with a 0.76 M DAP solution. On the left, pseudo-amorphous coating formed on micritic dolomite and incipient formation of spherical structures in an elongated arrangement (white rectangle); on the right, big dolomitic crystal with the overgrowth of crystal agglomerates in spherical structures, some of them having prismatic elongations; (c) treated Angera stone after the poultice with a 3.00 M DAP solution, showing detail of spherical crystallites and their aggregation in chains - elongated arrangement (arrows).

189 3.3. Evidence of HAP formation by thermal treatments

190 Thermal treatments are an acknowledged tool to investigate the nature of calcium phosphate phases
191 showing at room conditions (rT) hardly distinguishable X-ray diffraction patterns [31], by promoting *T*-induced
192 phase transitions.

193 More specifically, heating of: i) poorly-crystalline stoichiometric HAP generates crystalline
194 stoichiometric HAP; ii) partially-substituted HAP (e.g., carbonated-hydroxyapatite) produced crystalline HAP
195 in mixture with β -tricalcium phosphate (β -TCP, β -Ca₃(PO₄)₂), and with β -TCP predominant vs HAP; iii) OCP
196 do not generates HAP, but only β -TCP in mixture with β -calcium pyrophosphate (β -CPP, Ca₂P₂O₇) [9,31].

197 Figure 3 shows the parent-to-product phase transformations occurred in Angera stone treated with the 0.76
198 M DAP solutions. Identical results are obtained on the specimens treated with the 3.00 M one. Thermal
199 treatments were carried out also on untreated Angera stone for comparison and the principal XRD patterns are
200 provided as well.

The heating at 400 °C induces the first phase variation, namely the total disappearance of the XRD peaks of struvite, due to the collapse of struvite into amorphous magnesium phosphate phases. Previous studies describe that heating induces a chain decomposition, involving the initial formation of amorphous magnesium hydrogen phosphate hydrate ($\text{MgHPO}_4 \cdot 3\text{H}_2\text{O}$ [36]), followed by its transformation into amorphous anhydrous magnesium hydrogen phosphate (MgHPO_4 [32,35,36]). In this study, it was not possible to discriminate between the two amorphous products, thus they are referred to a generic amorphous magnesium phosphate phases.

The heating at 600 °C acts on poorly-crystalline calcium phosphates, as the weak broad peak at $\sim 25.90^\circ$ of 2 Theta becomes more pronounced. The principal phase transformation occurs after heating at 900 °C, where dolomite of the substrate is decomposed into magnesium oxide (MgO , peaks at 42.92° and 62.30°) and lime (CaO , peaks at 32.27° , 37.48° and 53.97° ; phase transformation probably occurred between 600-820 °C [33,34]) and the peaks of calcium phosphates become more defined. More precisely, the growth of sharp, well-defined peaks at 2 Theta of 25.90° (d_{002}), 31.77° (d_{211}), 32.96° (d_{300}) and 34.08° (d_{202}) unambiguously identify crystalline HAP as heating by-product. Only the very weak peak at 28.09° could be attributed to β -TCP.

Magnesium oxide and lime, the calcinations by-products of dolomite, are active components that might interact with the calcium phosphates at high temperature, resulting in a further calcium source. However, even if the occurrence of this phenomenon cannot be *a priori* excluded, there is no evidence of other high-temperature calcium phosphate phases nor of high-temperature magnesium phosphates formed by the reaction of active oxides with amorphous phosphates.

These results demonstrate that apatite formed after DAP treatments is poorly-crystalline but mainly stoichiometric. The formation of minor fraction of β -TCP indicates that a partially-substituted nonstoichiometric apatite and OCP are formed as well by the DAP treatment, but with poorly-crystalline stoichiometric HAP predominant versus these phases.

No phase variations are observed for silicates and phyllosilicates of the Angera stone matrix.

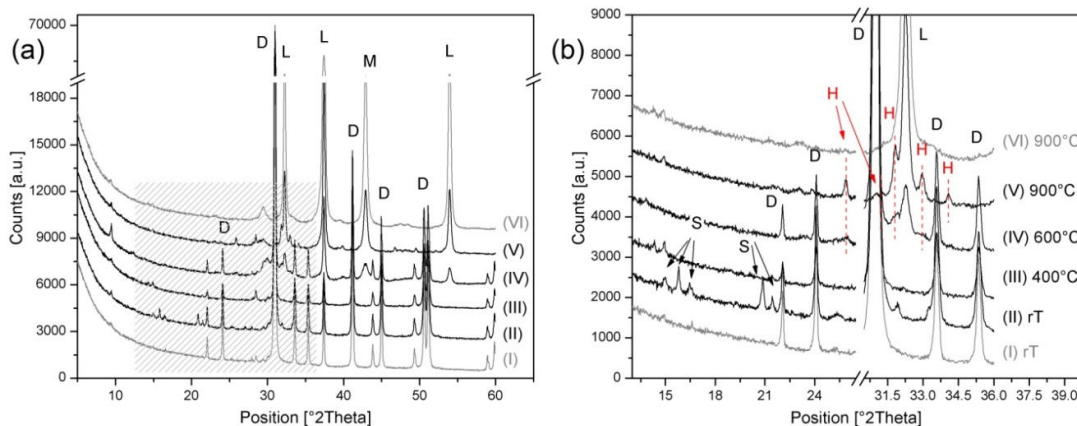


Figure 3. (a) XRD patterns of untreated (grey patterns) and treated (black patterns) Angera stone at room temperature (rT) and after heating at 400 °C, 600 °C and 900 °C. (b) zoom of (a) showing the phase transformation occurred with heating. D = dolomite, L = lime, M = MgO, S = struvite, H = hydroxyapatite.

4. Discussion

The DAP reaction with the Angera stone involves the partial dissolution of the dolomite grains, with the release of calcium and magnesium ions from the stone substrate. It is followed by the interaction of these bivalent ions with the reagent ions, with the consequent nucleation and growth of newly-formed phosphate phases. This dissolution - recrystallization process is topotactic and forms magnesium phosphates and calcium phosphates: (struvite and hydroxyapatite, respectively) arranged in a coating on dolomite grains. The micro-morphology of this coating, which resembles almost the features of polymeric products used for the conservation, is actually quite different from the crystalline *shell* observed on calcite-based lithotypes [9,10], even where the reaction occurred in presence of Mg-containing veins [9,16,17]. The crystallization of these phases is not merely a superficial film, but it is a binding network which connects different dolomite grains.

241 The crystallization of the newly-formed phosphates is influenced by the microstructure and the
242 composition of the lithotype. In particular, the microstructure of the substrate acts on the micro-morphology of
243 the new phases. In fact, the newly-formed phosphates are well shaped when they grow on dolomite in large
244 crystals, while on micritic dolomite the phosphates mainly develop tiny crystals with irregular morphologies.

245 Mg-phosphates are crystalline, as demonstrated by the sharp well-defined XRD peaks of struvite. On the
246 contrary, the apatite is formed as poorly ordered partially-substituted crystals. It is worth underlying that
247 hydroxyapatite formed after DAP treatments by using only calcium ions of the substrate is never highly
248 crystalline, even when the reaction occurs on calcium carbonate stones. However, the DAP reaction on
249 dolomite of Angera stone is particularly non-stoichiometric, and the formed apatite is so poorly ordered that its
250 identification before heating is assumed only by a weak broad XRD peak. It is conceivable that Mg^{2+} ions
251 destabilizes the crystalline structure and growth sequence of apatite, that shows a morphology characterized by
252 an amorphous-spherical aspect similar to that reported by Ren *et al.* [43]. In any case, the thermal treatments
253 shed light on the nature of this phase and, for clarity's sake, the poorly ordered calcium phosphate phase formed
254 after the DAP treatment will be labelled as HAP in the following discussion.

255 The HAP X-ray diffraction peak is more intense in the specimens treated with the DAP 0.76 M, while
256 struvite peaks are more evident in the specimens treated with the DAP 3.00 M, even though it is only a
257 semi-quantitative evaluation. The higher is the DAP molarity, the higher is the ion dissolution from the
258 substrate; consequently, the more pronounced is the formation of struvite and the more poorly crystalline is
259 HAP. Regarding to the DAP molarity, the "coating-like" morphology is more evident in the specimens treated
260 with the DAP 0.76 M, whereas the rounded morphology in elongated chains is prevalent on the specimens
261 treated with the DAP 3.00 M. Considering these features, it is conceivable to hypothesize that these
262 morphological and compositional differences depends on the reaction variables, first of all the pH and the ionic
263 strength. Moreover, dolomite is less reactive than calcite to DAP solutions [20], thus the reaction kinetic may be
264 different as well.

265 The minimum solubility of struvite is documented in the pH range 9-11 [42], while HAP crystallize in
266 aqueous solutions at pH >8.5-9 [14].

267 At the beginning of the reaction the pH is 8.8, which is close to the ideal crystallization pH for both the
268 phases. Actually, even though it is not possible to measure the evolution of pH on grain boundaries, it is
269 reasonable that pH decreases as long as the reaction evolves, due to the: i) dissociation of the reagent into PO_4^{3-}
270 and H^+ ions [9,44], ii) nucleation of HAP which consumes OH^- ions [41]; iii) precipitation of struvite which
271 subtract NH_4^+ ions [36].

272 Furthermore, close to dolomite boundaries where the dissolution-recrystallization process is ongoing, Ca^{2+}
273 and Mg^{2+} ions compete for PO_4^{3-} groups to nucleate calcium phosphates or magnesium phosphates. In the
274 microscale variations of the pH and of the ionic strength at the grain boundaries, carbonate and bicarbonate ions
275 are reasonably involved as well [45].

276 The prediction of struvite/apatite crystallization is particularly challenging when this reaction occurs on
277 dolomite stone. A combination of conditions governed by thermodynamics of solid-liquid equilibrium, kinetics
278 of reaction, pH of the solution from which struvite and hydroxyapatite may precipitate, super saturation and
279 presence of foreign ions influence their nucleation and crystallisation process.

280 In particular, the influence of foreign ions on struvite/hydroxyapatite nucleation and their crystallisation is
281 a crucial issue because of Ca and Mg are at the same time "impurities" in that solution from which the two
282 Mg/Ca phosphate phases may precipitate. This mutual interference affects the growth rate, which in turn
283 inhibits the increase of crystal size [36].

284 This complex ionic equilibrium, with pH fluctuations toward not ideal reaction conditions, generates two
285 effects. The first one is a clear inhibiting effect of Mg^{2+} ions on the crystallinity, morphology and crystal size of
286 HAP, which nucleates as a poorly-crystalline phase and with a pseudo-amorphous coating aspect or in
287 agglomerated structures (depending on the employed DAP molarity). A partial intra-crystalline Mg^{2+} vs. Ca^{2+}
288 substitution, as ab initio simulated by [43], is also possible. Referring to previous findings, this phenomenon
289 should induce a slight variation of the unit-cell constants. In the case of HAP formed after the DAP treatment on
290 dolomite, the possible generation of a Mg-HAP is not clearly documented, as it is most likely a very minor
291 phase.

292 The second aspects is the interference of Ca^{2+} ions in the crystallization of struvite, which occurred in
293 sub-micrometric nuclei of crystals, more than well structured micrometric prismatic crystallites. The possible
294 presence of ions substitutions in struvite is also highly likely size [36].

295 Focusing on conservation evaluations, the newly-formed crystalline phases nucleate in a coating on
 296 dolomite grains by forming a covering which provides new functional properties to the substrate.

297 Irrespective by their composition, the newly-formed phases nucleate on the dolomite grain surface and
 298 among dolomite grains, hence their crystallization provide a clear bonding action on the stone microstructure.
 299 Further experiments are scheduled in order to explore the quantitative ratio of the two phases and their
 300 arrangement within the stone pores.
 301

302 5. Conclusions

303 The DAP reaction with polycrystalline dolomite of the Angera stone determines an interaction among
 304 calcium and magnesium ions, which compete each other to form phosphate phases. The variation of the solution
 305 pH and of the ionic strength during the DAP reaction with dolomite generate a complex crystallization
 306 processes of the phosphate phases, which are formed as Mg-phosphates and Ca-phosphates crystals with
 307 morphologies different from those commonly described in literature. The mutual interference of the ions
 308 involved in reaction (NH_4^+ , Mg^{2+} , PO_4^{3-} , Ca^{2+} , CO_3^{2-} , HCO_3^-) determines an irregular crystal growth pattern
 309 with respect to the primary nucleation process. The consequence is a clear effect in the crystallization of the new
 310 phases (struvite and hydroxyapatite) in terms of crystal size, micro-morphology, composition and crystallinity.

311 In particular, the Mg^{2+} ions presence destabilizes the hydroxyapatite well-ordered structure, causing a
 312 structural variation that inhibits the growth of well-shaped crystals and, on the contrary, promotes the formation
 313 of an amorphous coating on the dolomite grains. The higher is the DAP molarity, the higher is the Mg molar
 314 fraction in the solution and then the lower is the crystallinity of the formed calcium phosphate. In any case,
 315 heating treatments demonstrated that the newly-formed apatite is poorly crystalline but mainly stoichiometric,
 316 thus with a Ca/P molar ratio quite close to the ideal one (1.67).

317 On the other hand, the struvite formation is affected by the presence of free calcium ions as well, and the
 318 descending effects are observed in the crystal morphology and crystal size.

319 Regarding the effects induced by the DAP treatment on the Angera lithotype, it is important to consider
 320 that the new phases formed on the dolomite grains create a crystalline network that likely improves the cohesion
 321 of the lithotype.
 322

323 **Author Contributions:** conceptualization, data curation, investigation, methodology, writing—original draft
 324 writing—review & editing, E. Possenti and C. Colombo; writing—review & editing, C. Conti; supervision, M. Realini and
 325 G. D. Gatta.

326

327 **Funding:** This research received no external funding

328

329 **Conflicts of Interest:** The authors declare no conflict of interest

330

331 References

- 332 1. Matteini, M.; Rescic, S.; Fratini, F.; Botticelli, G. Ammonium Phosphates as Consolidating Agents for Carbonatic
 333 Stone Materials Used in Architecture and Cultural Heritage: Preliminary Research. *Int. J. Archit. Herit. Conserv.*
 334 *Anal. Restor.* **2011**, *5*, 717–736, doi:10.1080/15583058.2010.495445.
- 335 2. Sassoni, E.; Naidu, S.; Scherer, G.W. The use of hydroxyapatite as a new inorganic consolidant for damaged
 336 carbonate stones. *J. Cult. Herit.* **2011**, *12*, 346–355, doi:10.1016/j.culher.2011.02.005.
- 337 3. Yang, F.; Zhang, B.; Liu, Y.; Wei, G.; Zhang, H.; Chen, W.; Xu, Z. Biomimic conservation of weathered
 338 calcareous stones by apatite. *New J. Chem.* **2011**, *35*, 887, doi:10.1039/c0nj00783h.
- 339 4. Matteini, M.; Colombo, C.; Botticelli, G.; Casati, M.; Conti, C.; Negrotti, R.; Realini, M.; Possenti, E. Ammonium
 340 phosphates to consolidate carbonatic stone materials: an inorganic-mineral treatment greatly promising. In *Built*
 341 *Heritage 2013 Monitoring Conservation Management*; 2013; pp. 1278–1286.
- 342 5. Ni, M.; Ratner, B.D. Nacre surface transformation to hydroxyapatite in a phosphate buffer solution. *Biomaterials*

- 343 **2003**, *24*, 4323–31, doi:10.1016/S0142-9612(03)00236-9.
- 344 6. Kasioptas, A.; Perdikouri, C.; Putnis, C. V.; Putnis, A. Pseudomorphic replacement of single calcium carbonate
345 crystals by polycrystalline apatite. *Mineral. Mag.* **2008**, *72*, 77–80, doi:10.1180/minmag.2008.072.1.77.
- 346 7. Sassoni, E. Hydroxyapatite and Other Calcium Phosphates for the Conservation of Cultural Heritage: A Review.
347 *Materials (Basel)*. **2018**, *11*, 557, doi:10.3390/ma11040557.
- 348 8. Sassoni, E.; D’Amen, E.; Roveri, N.; Scherer, G.W.; Franzoni, E. Durable self-cleaning coatings for architectural
349 surfaces by incorporation of TiO₂ nano-particles into hydroxyapatite films. *Materials (Basel)*. **2018**, *11*, 1–16,
350 doi:10.3390/ma11020177.
- 351 9. Possenti, E.; Colombo, C.; Conti, C.; Gigli, L.; Merlini, M.; Plaisier, J.R.; Realini, M.; Sali, D.; Gatta, G.D.
352 Diammonium hydrogenphosphate for the consolidation of building materials. Investigation of newly-formed
353 calcium phosphates. *Constr. Build. Mater.* **2019**, *195*, 557–563, doi:10.1016/j.conbuildmat.2018.11.077.
- 354 10. Possenti, E.; Colombo, C.; Bersani, D.; Bertasa, M.; Botteon, A.; Conti, C.; Lottici, P.P.; Realini, M. New insight
355 on the interaction of diammonium hydrogenphosphate conservation treatment with carbonatic substrates: A
356 multi-analytical approach. *Microchem. J.* **2016**, *127*, 79–86, doi:10.1016/j.microc.2016.02.008.
- 357 11. Molina, E.; Rueda-Quero, L.; Benavente, D.; Burgos-Cara, A.; Ruiz-Agudo, E.; Cultrone, G. Gypsum crust as a
358 source of calcium for the consolidation of carbonate stones using a calcium phosphate-based consolidant. *Constr.*
359 *Build. Mater.* **2017**, *143*, 298–311, doi:10.1016/j.conbuildmat.2017.03.155.
- 360 12. Sassoni, E.; Graziani, G.; Franzoni, E. Repair of sugaring marble by ammonium phosphate: Comparison with ethyl
361 silicate and ammonium oxalate and pilot application to historic artifact. *Mater. Des.* **2015**, *88*, 1145–1157,
362 doi:10.1016/j.matdes.2015.09.101.
- 363 13. Wang, L.; Nancollas, G.H. Calcium Orthophosphates: Crystallization and Dissolution. *Chem. Rev.* **2008**, *108*,
364 4628–4669, doi:10.1021/cr0782574.Calcium.
- 365 14. Dorozhkin, S. V. Calcium orthophosphates. *J. Mater. Sci.* **2007**, *42*, 1061–1095, doi:10.1007/s10853-006-1467-8.
- 366 15. Calore, N.; Botteon, A.; Colombo, C.; Comunian, A.; Possenti, E.; Realini, M.; Sali, D.; Conti, C. High Resolution
367 ATR μ -FTIR to map the diffusion of conservation treatments applied to painted plasters. *Vib. Spectrosc.* **2018**, *98*,
368 105–110, doi:10.1016/j.vibspec.2018.07.012.
- 369 16. Possenti, E. Inorganic products used in the Conservation of Cultural Heritage: interaction with carbonatic
370 substrates and newly-formed crystalline phases, PhD Thesis, University of Milan, Milan, Italy, 2019, February 7th.
- 371 17. Possenti, E.; Colombo, C.; Conti, C.; Gigli, L.; Merlini, M.; Plaisier, J.R.; Realini, M.; Gatta, G.D. Grazing
372 incidence synchrotron X-ray diffraction of marbles consolidated with diammonium hydrogen phosphate
373 treatments: non-destructive probing of buried minerals. *Appl. Phys. A* **2018**, *124*, 383,
374 doi:10.1007/s00339-018-1798-8.
- 375 18. Possenti, E.; Colombo, C.; Conti, C.; Gigli, L.; Merlini, M.; Plaisier, J.R.; Realini, M.; Gatta, G.D. What’s
376 underneath? A non-destructive depth profile of painted stratigraphies by synchrotron grazing incidence X-ray
377 diffraction. *Analyst* **2018**, *143*, 4290–4297, doi:10.1039/C8AN00901E.
- 378 19. Gulotta, D.; Bertoldi, M.; Bortolotto, S.; Fermo, P.; Piazzalunga, A.; Toniolo, L. The Angera stone. A challenging
379 conservation issue in the polluted environment of Milan (Italy). *Environ. Earth Sci.* **2013**, *69*, 1085–1094,
380 doi:10.1007/s12665-012-2165-2.
- 381 20. Schultheiss, S.; Sethmann, I.; Schlosser, M.; Kleebe, H.-J. Pseudomorphic transformation of Ca/Mg carbonates
382 into phosphates with focus on dolomite conversion. *Mineral. Mag.* **2013**, *77*, 2725–2737,
383 doi:10.1180/minmag.2013.077.6.03.
- 384 21. Pesonen, J.; Myllymäki, P.; Verweken, G.; Hu, T.; Prokkola, H.; Tuomikoski, S. Use of calcined dolomite as
385 chemical coagulant in the simultaneous removal of nitrogen and phosphorus. In *6th International Conference on*
386 *Sustainable Solid Waste Management*; Naxos, 2018; pp. 1–8.

- 387 22. Beeson, K.C. Chemical Reactions in Fertilizer Mixtures Reactions of Diammonium Phosphate with Limestone and
388 with Dolomite. *Ind. Eng. Chem.* **1937**, *29*, 705–708, doi:10.1021/ie50330a025.
- 389 23. Keenen, F.G.; Morgan, W.A. Rate of Dolomite Reactions in Mixed Fertilizers. *Ind. Eng. Chem.* **1937**, *29*, 197–201,
390 doi:10.1021/ie50326a020.
- 391 24. Cavallo, A.; Bigioggero, B.; Colombo, A.; Tunesi, A. The Verbano Cusio Ossola province: A land of quarries in
392 northern Italy (Piedmont). *Period. di Mineral.* **2004**, *73*, 197–210.
- 393 25. Alessandrini, G.; Bugini, R.; Peruzzi, R. I materiali lapidei impiegati nei monumenti lombardi e i loro problemi di
394 conservazione. In *Materiali lapidei*; 1987; pp. 145–156.
- 395 26. Alessandrini, G. Le pietre del monumento. In *La Ca' Granda di Milano. L'intervento conservativo sul cortile*
396 *richiniano*; Pizzi, A., Ed.; Milano, 1993; pp. 173–203 ISBN 88-366-0435-8.
- 397 27. Alessandrini, G. Lo stato di conservazione dei materiali lapidei: morfologia e cause di degrado. In *La Ca' Granda*
398 *di Milano. L'intervento conservativo sul cortile richiniano*; Pizzi, A., Ed.; 1993; pp. 219–239 ISBN
399 88-366-0435-8.
- 400 28. Riganti, V.; Rosetti, R.; Soggetti, F.; Veniale, F.; Zezza, U. *Alterazione e protezione delle pietre dei monumenti*
401 *storici dell'Università di Pavia*; Pavia, 1978;
- 402 29. Pittaluga, D.; Fratini, F.; Nielsen, A.; Rescic, S. Industrial archaeological sites and architectonic remains: the
403 problem of consolidation in humid areas. In *Scienza e Beni Culturali XXVIII*; Arcadia Ricerche, Ed.; 2012; pp.
404 303–312.
- 405 30. Sassoni, E. Phosphate-based treatments for conservation of stone. *RILEM Tech. Lett.* **2017**, *2*, 14,
406 doi:10.21809/rilemtechlett.2017.34.
- 407 31. Karampas, I.A.; Kontoyannis, C.G. Characterization of calcium phosphates mixtures. *Vib. Spectrosc.* **2013**, *64*,
408 126–133, doi:10.1016/j.vibspec.2012.11.003.
- 409 32. Bhuiyan, M.I.H.; Mavinic, D.S.; Koch, F.A. Thermal decomposition of struvite and its phase transition.
410 *Chemosphere* **2008**, *70*, 1347–56, doi:10.1016/j.chemosphere.2007.09.056.
- 411 33. Gunasekaran, S.; Anbalagan, G. Thermal decomposition of natural dolomite. *Bull. Mater. Sci.* **2007**, *30*, 339–344,
412 doi:10.1007/s12034-007-0056-z.
- 413 34. Olszak-Humienik, M.; Jablonski, M. Thermal behavior of natural dolomite. *J. Therm. Anal. Calorim.* **2015**, *119*,
414 2239–2248, doi:10.1007/s10973-014-4301-6.
- 415 35. Ramlogan, M. V.; Rouff, A.A. An investigation of the thermal behavior of magnesium ammonium phosphate
416 hexahydrate. *J. Therm. Anal. Calorim.* **2016**, *123*, 145–152, doi:10.1007/s10973-015-4860-1.
- 417 36. Tansel, B.; Lunn, G.; Monje, O. Struvite formation and decomposition characteristics for ammonia and phosphorus
418 recovery: A review of magnesium-ammonia-phosphate interactions. *Chemosphere* **2018**, *194*, 504–514,
419 doi:10.1016/j.chemosphere.2017.12.004.
- 420 37. Koutsopoulos, S. Synthesis and characterization of hydroxyapatite crystals: a review study on the analytical
421 methods. *J. Biomed. Mater. Res.* **2002**, *62*, 600–12, doi:10.1002/jbm.10280.
- 422 38. Dorozhkin, S. V. Amorphous calcium (ortho)phosphates. *Acta Biomater.* **2010**, *6*, 4457–4475,
423 doi:10.1016/j.actbio.2010.06.031.
- 424 39. Dorozhkin, S. V. Calcium Orthophosphates in Nature, Biology and Medicine. *Materials (Basel)*. **2009**, *2*, 399–498,
425 doi:10.3390/ma2020399.
- 426 40. Elliott, J.C. Hydroxyapatite and Nonstoichiometric Apatites. In *Structure and Chemistry of the Apatites and Other*
427 *Calcium Orthophosphates*; 1994; pp. 111–189.
- 428 41. Drouet, C. Apatite formation: Why it may not work as planned, and how to conclusively identify apatite
429 compounds. *Biomed Res. Int.* **2013**, *2013*, 1–12, doi:10.1155/2013/490946.
- 430 42. Ariyanto, E.; Ha Ming, A.; Tushar, S. Effect of initial solution pH on solubility and morphology of struvite

- 431 crystals. In *CHEMECA Conference*; 2011; pp. 1–10.
- 432 43. Ren, F.; Leng, Y.; Xin, R.; Ge, X. Synthesis, characterization and ab initio simulation of magnesium-substituted
433 hydroxyapatite. *Acta Biomater.* **2010**, *6*, 2787–2796, doi:10.1016/j.actbio.2009.12.044.
- 434 44. Naidu, S.; Scherer, G.W. Nucleation, growth and evolution of calcium phosphate films on calcite. *J. Colloid*
435 *Interface Sci.* **2014**, *435*, 128–137, doi:10.1016/j.jcis.2014.08.018.
- 436 45. Cao, X.; Harris, W. Carbonate and magnesium interactive effect on calcium phosphate precipitation. *Environ. Sci.*
437 *Technol.* **2008**, *42*, 436–442.
- 438